CONF-900466--12

58307-00-105

CONF-900466--12

DE90 010053

ATOMIC STRUCTURE OF Ag/Ni INTERFACES*

Y. Gao and K. L. Merkle
Materials Science Division
Argonne National Laboratory
Argonne, IL 60439

MARCH 1990

*This work was supported by the U.S. Department of Energy, BES Materials Sciences, under Contract W-31-109-ENG-38.

To be submitted for the MRS meeting to be held April 16-21, 1990, San Francisco, California

---

ATOMIC STRUCTURE OF Ag/Ni INTERFACES

Y. GAO and K. L. MERKLE
Materials Science Division, Argonne National Laboratory, Argonne, IL 60439

ABSTRACT

While in heterophase systems of small lattice parameter differences, misfit dislocations are often formed at the interface, it is not known, whether and in which form, misfit localization occurs when the misfit is very large. The atomic structure of Ag/Ni interfaces (misfit 14%) was studied by high-resolution electron microscopy (HREM). A special technique was developed to prepare interface specimens suitable for HREM observations.

Lattice statics calculations, using embedded-atom potentials, were performed to determine the structure and energies of Ag/Ni interfaces. The lowest interfacial energy was found for the cube-on-cube orientation and (111) interfaces. This is in agreement with the experimental observation, that all interfaces are strongly faceted with (111)Ag/(111)Ni facets.

Misfit localization was found by HREM and computer simulation. The HREM observations will be compared to images derived from image simulations, based on model structures obtained from embedded atom calculations.

INTRODUCTION

It is well known that in heterophase systems of small lattice parameter difference, misfit dislocations often exist at the interface, forming a semi-coherent interface [1]. However, it is generally not known, whether or not, and in which form misfit localization occurs when the misfit is very large. Recently, low-energy Ag/Ni interfaces have been investigated by lattice statics calculations and crystallite rotation experiments [2,3]. The results of the crystallite rotation experiments indicate that the lattice statics calculations using embedded atom potentials [4] are able to predict the existence of low-energy interfaces in the Ag/Ni system. However, the semi-coherent interface configuration implied by these calculations has not been confirmed by experimental observation.

The Ag/Ni system chosen in the present investigation can be used as a model system for metal/metal interfaces because of the absence of mutual solid solubility and intermetallic compound formation [5], and because of available results of the atomistic calculations. In order to obtain suitable specimens for high-resolution electron microscopy (HREM) observation a special technique for the preparation of well-characterized Ag/Ni interfaces was developed. Briefly, composite epitaxial thin films, consisting of Ni particles embedded in the Ag matrix, were used. This technique has several very useful features: 1) a common low-index zone axis between particles and the matrix is easily achieved, and thus HREM studies are possible; 2) information on low-energy interfaces can be obtained from the faceting of the particles; and 3) different kinds of interfaces such as metal/metal, metal/alloy and metal/metal-oxide can be studied on the same film [6].

In this paper, we describe our initial HREM observations for the study of the atomic structure of the Ag/Ni interfaces. In all cases we find a tendency towards maintaining coherence between low-index atomic planes crossing the interface. The results also indicate that the large misfit between Ag and Ni (~14%) is accommodated by misfit dislocations at the interfaces, forming semi-coherent interfaces, and the lowest interfacial energy is found in the (111)Ag/(111)Ni interface. Comparison of the observed images with simulated images, based on the relaxed structure obtained from lattice statics calculations, [3] will also be made for the (111)Ag/(111)Ni interface.

EXPERIMENTAL AND COMPUTATIONAL PROCEDURES

The TEM sample preparation of heterophase interfaces, in systems that do not allow the formation of suitable precipitates, usually starts out from a macroscopic interface which was formed by an appropriate bonding process. An edge-on view of the interface, at high resolution, can only be obtained by cross-sectional sample preparation techniques. The latter generally involve rather lengthy mechanical and sputter-thinning processes, which, moreover, not always result in the desired thin sections $\leq$ 10 nm, that are needed for HREM observation. The following procedure, which avoids the cross-sectional sample preparation, but results in a great number of suitably thin, well aligned, edge-on interfaces, was developed for the purpose of the present investigations.

Ag/Ni composite thin films were prepared by electron-beam evaporation using the following procedure. A silver film with a thickness of 80 nm was deposited epitaxially on a (110) NaCl substrate held at 320 ^{o}C. The Ag film was then annealed on its substrate in vacuum at 400 ^{o}C for one half hour and cooled down to 300 ^{o}C. After annealing, the Ag film became largely continuous and smooth, but contained a number of small holes. The size of these holes ranged from 5 nm to 500 nm in diameter. Subsequently, Ni was deposited onto the Ag film, and the Ni film also grew epitaxially on the Ag film with an average thickness of about 40 nm. The Ni film was continuous and filled out the small holes in the Ag film. After removal from the vacuum chamber, the Ag/Ni film was annealed on its substrate in Ar + 10% H_2 at 500 ^{o}C for 20 minutes. The purpose of this annealing step was to form a strong bond between Ag and Ni, and to obtain the equilibrium interfacial structure. In addition, the anneal in the reducing atmosphere can eliminate any oxides formed during and after deposition. The NaCl substrate was then dissolved in water and the Ag/Ni film was picked up on a Ag TEM grid. The final specimens for HREM observations were prepared by argon ion-beam thinning to remove the Ni layer and to obtain thin areas with thickness less than 10 nm. A liquid-nitrogen-cooled stage was used during ion thinning. Because of the difference in original thickness between Ag/Ni and Ni layers, the thickness on the Ni side was always slightly smaller than that on the Ag side, even though the thinning rate for Ni is lower than that for Ag. The electron microscopy was performed using a Hitachi 9000, operated at 300 kV, at Northwestern University. All HREM images were obtained at close to axial illumination for several defocus values near the optimum focus condition.

Image simulations were performed using the multislice method implemented in the EMS program package developed by Stadelmann [7]. The relaxed structure of the (111)Ag/Ni interface was obtained from atomistic calculations [3]. A three-dimensional atomic model (3.30x3.07x1.74 nm) of the Ag/Ni bicrystal was cut from the relaxed structure in such a way that the bicrystal contained seven (111) lattice planes in each crystal along the interface normal, which corresponds to 3.07 nm. In the plane of the interface, the periodicity length is 3.30 nm in the direction of [1,-1,2], and 1.74 nm in the direction of [110]. The atomic model was then aligned such that the [110] direction was parallel to the electron beam. Multislice calculations with dynamical scattering arrays of 512x512 reciprocal lattice points were performed on these layers until the proper film thickness was achieved. The electron-wave-field computations were followed by image calculations for several thickness and defocus values.

RESULTS AND DISCUSSION

A typical Ni particle in the Ag matrix is shown in Fig. 1 which demonstrates that the Ni particles are strongly faceted. The selected-area electron diffraction pattern inset in Fig. 1 indicates a perfect cube-on-cube orientation relationship between the Ag matrix and the Ni particle. All faces of this Ni particle are parallel to the close-packed (111) lattice planes, which indicates that the (111)Ag/(111)Ni interfaces possess the lowest interfacial energy in the Ag/Ni system. This observation confirms the prediction by lattice statics calculations [3].

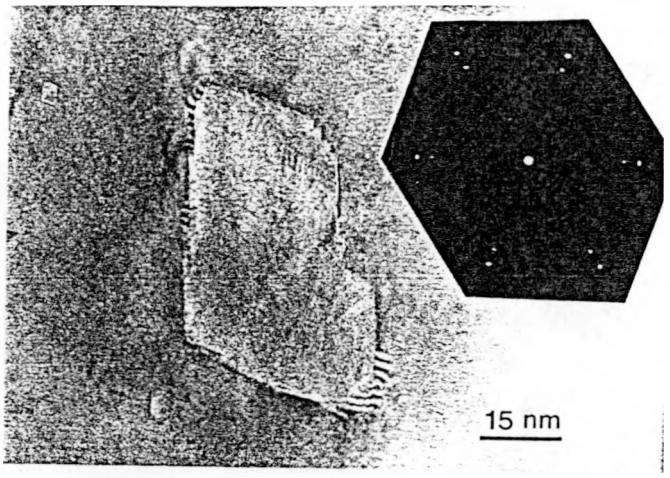

Fig. 1 A bright field image of a typical Ni particle in the Ag matrix. Inset diffraction pattern indicates the cube-on-cube orientation between Ni and Ag.

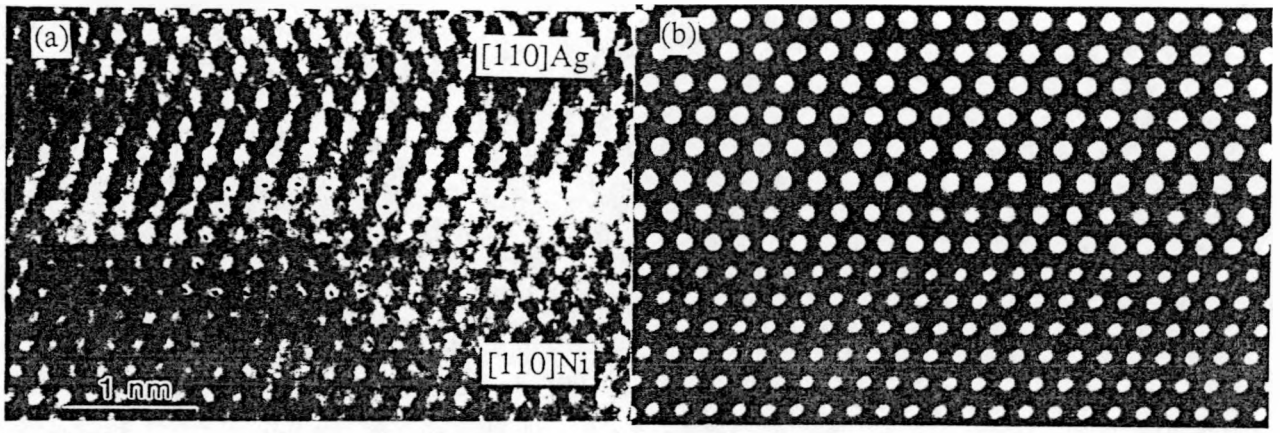

Fig. 2 (a) HREM image of a small segment of the (111)Ag/(111)Ni interface; (b) simulated image with t = 7.0 nm and Δf = -70.0 nm.

A representative HREM image of the (111)Ag/(111)Ni interface is given in Fig. 2(a). It is apparent that the interface is quite well connected with no evidence for the formation of an intermediate layer or a second phase at the interface. Several misfit dislocations can be observed at the interface. The average repeat distance of such misfit dislocations is found to be close to the projection of $6d_{(111)Ag}$ spacings or $7d_{(111)Ni}$ spacings along the [1,-1,2] direction, which is in agreement with the calculated value from a hard sphere model of the interface structure. The dislocation cores appear to be somewhat delocalized. However, in contrast to an incoherent interface, the (1,-1,1) planes outside the cores clearly are elastically continuous across the interface, forming a semi-coherent interface. A Burger's circuit was performed around a dislocation core as shown by the dot loop in Fig. 2a, indicating a Burger's vector **b** = a/2[110].

Fig. 2(b) represents the computer simulated image based on the relaxed model of the (111) Ag/Ni interface for a thickness t = 7.0 nm and defocus Δf = -70.0 nm. The metal columns are imaged as white dots, as in Fig. 2(a). It is clearly seen that the misfit dislocation cores also appear delocalized as shown in Fig. 2(a). By comparing the images in Figs. 2(a) and 2(b), it can be seen that the simulated image matches reasonably well with the observed image. It has been found that the largest relaxation distance near the dislocation cores in Ag is only about 5% of the Ag-Ag distance [3]. Therefore, complete localization at the misfit dislocations can not be achieved. This is also observed in Fig. 2(a). An apparent delocalization of the dislocation cores in HREM images can also be due to the finite thickness of the Ag/Ni films. Since the dislocations in the plane of the interface form a hexagonal dislocation network, the atomic relaxations differ from atom to atom in the same column throughout the thickness of the film, sometimes in opposite directions [3]. Thus, the imaged relaxations represent an average through the thickness, leading to a somewhat diffuse appearance of atomic columns (see Fig. 2b).

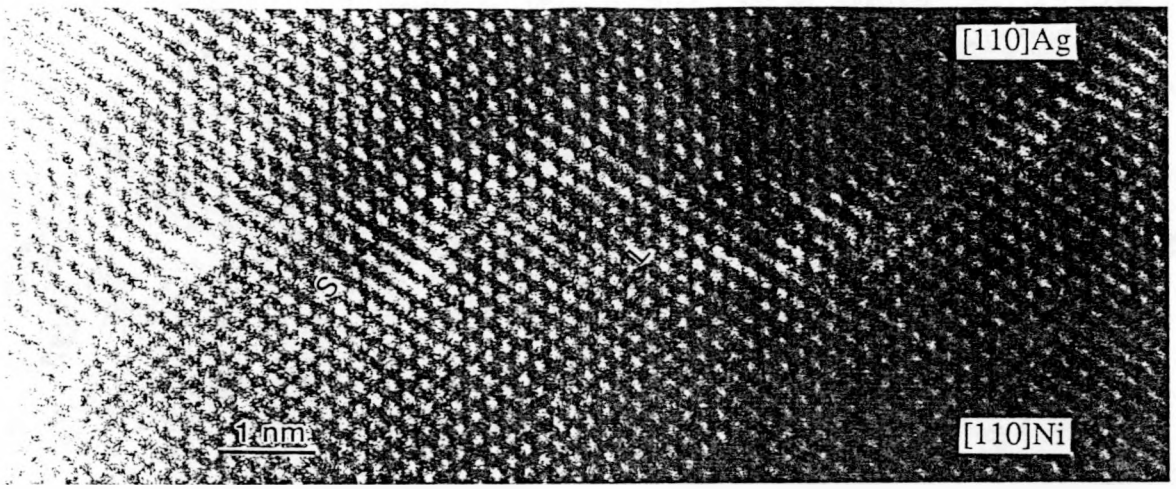

Fig. 3 A stepped interface is shown, which contains a coarse step without dislocation character (indicated by the letter S), and a step with dislocation character (L).

It is also noted that the misfit dislocation cores lie exactly in the plane of the Ag/Ni interfaces. There is no "standoff" effect at the interfaces. However, the "standoff" effect is commonly observed in metal/ceramics interfaces such as in the Nb/Al_2O_3 interface [8] and in the Ag/NiO interface [6]. Since the "standoff" effect is a result of a balance between the image force and coherency force due to different shear moduli of the two materials at the interface, a "standoff" distance of the dislocation cores from the interface should exist in the Ag/Ni system. However, the misfit dislocation in the Ag/Ni system is located in Ni, the hard material, which is different from the cases of the Nb/Al_2O_3 and Ag/NiO interfaces. Because of the absence of mutual solid solubility in the Ag/Ni system, it becomes impossible for the dislocation to cross the interface by the image force. Thus, it is concluded that there should be no "standoff" effect at any interface, formed by two insoluble materials, where the misfit dislocations are located in the hard material.

Interfacial steps were also observed in lattice images, although the interfaces generally were planar with a (111) habit plane. The location and the size of these steps were dependent on the Ni particle size and shape. The steps with a unit height were observed at the straight interfaces while most steps with a larger height were found at curved interfaces near large Ni particle corners. That is, the curved interfaces were faceted by well-defined steps on an atomic scale. Fig. 3 shows an example of such a faceted interface. The image clearly shows that the flat faces of the facets are (111)Ag/(111)Ni and the coarse steps exhibit strain contrast. The steps are exactly parallel to the <110> direction of projection, and the unit of the step height corresponds to the spacing of close-packed (111) lattice planes. A coarse step with a height less than one misfit dislocation spacing is shown in Fig. 3, as marked by a letter S. It is clearly seen that no misfit dislocation is observed at the step. However, if the step height is larger than one dislocation spacing, a dislocation should be formed in order to reduce the coherency strain energy at the interface. An example of such a dislocation is presented in Fig. 3, indicated by L.

To investigate structural details of the facets, lattice images were recorded for a number of faceted interfaces. Fig. 4(a) shows the strong tendency of a curved interface at a large Ni particle corner to facet along (111)Ag/(111)Ni. The curved interface is faceted with a number of steps. However, in contrast to this, sharp corners without steps were observed for small Ni particles. Fig. 4(b) shows an example of such faceting with a shape angle about 125°. The interface at one side of the corner is formed by (111)Ag/(111)Ni while the interface at the other side is (001)Ag/(001)Ni. It is noted that there apparently is no strong strain contrast at the (111)Ag/(111)Ni interface while strong strain contrast appears at the (001)Ag/(001)Ni interface. Fig. 5 depicts a (011)Ag/(011)Ni interface with strong (111) faceting. These facets are also formed with (111)Ag/(111)Ni, and show a "saw-tooth" morphology.

The strong faceting of the Ag/Ni interfaces on a large scale (Fig. 1) as well as on an atomic scale (Figs. 4 and 5), confirms the prediction of lattice statics calculations [3] that the (111)Ag/(111)Ni interface has the lowest interfacial energy in the Ag/Ni system. This confirmation is not only from a qualitative point of view, but also from a semi-quantitative point of view. It is noted that the (011)Ag/(011)Ni interface in Fig. 5 is strongly faceted with (111)Ag/(111)Ni interfaces. This represents a 23 % increase in the total interfacial area, compared to a flat (011) interface. Therefore, the interfacial energy of the (111)Ag/(111)Ni interface has be to lower than that of the (011)Ag/(011)Ni interface by 19% if decomposition into (111) facets is favored energetically. The interfacial energy of the (111)Ag/(111)Ni interface was calculated as 417 mJm^{-2} while the interfacial energy of the (011)Ag/(011)Ni interface as 828 mJm^{-2} [3]. Thus a substantial decrease in total interfacial energy of the (011)Ag/(011)Ni interface is accomplished by forming (111) facets.

CONCLUSIONS

The present HREM observations lead to the following conclusions. The large misfit at the Ag/Ni interfaces is accommodated by misfit dislocations. The dislocations lie exactly at the interfaces without any standoff distance. The observed dislocation spacing is in good agreement with the calculated value. All Ag/Ni interfaces are strongly faceted with (111)Ag/(111)Ni facets, which indicates that the interfacial energy of the (111)Ag/(111)Ni interfaces is lowest in the Ag/Ni system. This confirms the predictions by the lattice statics calculations, using the embedded atom method. Finally, clean and well-characterized interfaces can be prepared by a special thin-film technique.

ACKNOWLEDGEMENTS

This work was supported by the U. S. Department of Energy, Basic Energy Sciences - Materials Science under contract No. W-31-109-ENG-38. The use of the H-9000 in the Dept. of Mater. Sci. & Eng., Northwestern University is gratefully acknowledged.

REFERENCES

1. J. W. Matthews, Ed., Epitaxial Growth, Academic Press, New York, NY (1975).
2. Y. Gao, S. A. Dregia and P. G. Shewmon, Acta metall. 37, 1627 (1989).
3. Y. Gao, P. G. Shewmon and S. A. Dregia, Acta metall. 37, 3165 (1989).
4. S. M. Foiles, M. I. Baskes, and M. S. Daw, Phys. Rev. B 33, 7983 (1986).
5. M, Singleton and P. Nash, Bull. Alloy Phase Diagr. 8, 119 (1987).
6. Y. Gao and K. Merkle, Submitted to J. of Mater. Res.
7. P. A. Stadelmann, Ultramicroscopy, 21, 131 (1987).
8. W. Mader, Mater. Res. Symp. Proc. 82, 403 (1987).